SSCL-N-788

Study of Energy Deposition in the SSC Corrector Elements for the Radiation Test Experiment with 200 MeV Protons at BNL

G. López

Superconducting Super Collider Laboratory*
2550 Beckleymeade Avenue
Dallas, Texas 75237

April 1992

* Operated by the Universities Research Association, Inc., for the U.S. Department of Energy under Contract No. DE-AC35-89ER40486.

SSCL-N-788

Study of Energy Deposition in the SSC Corrector Elements for the Radiation Test Experiment with 200 MeV Protons at BNL

G. López

Abstract

The MARS10 Monte Carlo program is used to estimate the energy deposition from 200 MeV protons in the superconducting dipole, quadrupole and sextupole SSC corrector elements. The study includes different incident angles of interaction with respect the beam pipe and different squared-beam sizes.

1.0 INTRODUCTION

Planned experiments using the Brookhaven National Laboratory (BNL) 200 MeV proton beam will study the behavior of superconducting corrector magnets under expected SSC ring radiation levels.[1] The magnets will be studied (quench, before and after warm-up and cool-down thermocycles) after radiation exposures of the hadronic equivalent radiation dose of the SSC. Additional experiments at similar radiation levels and low temperatures will study the properties (stress, electrical conductivity, etc.) of materials that could be used for the construction of the corrector magnets. At the test energy level, the energy deposition is mainly due to ionization, a small amount from nuclear excitation, and none from the electromagnetic (photons-electrons shower) component. However, during normal SSC operation about 30% of the expected energy deposited in these magnets will be from the hadronic shower component and 70% from the electromagnetic shower.[2] In a typical beam-gas scattering event, this major electromagnetic component is due mainly to the large amount of photons with energies below 4 TeV which appear from π° decay as shown in Figure 1. The resulting hadronic dose of this experiment will be compared with the respective component for the SSC operational radiation levels. However, there is no similar comparison of the electromagnetic component because a gamma or electron source machine would be needed. These experiments also do not consider the quench level for the corrector magnets under spilling protons—an issue which will require study once the SSC prototypes are selected.

Estimates of hadronic shower energy deposition in the coil are needed to select certain parameters such as incident angle, beam profile size, and radiation dose. This estimation is done with the "inclusive" Monte Carlo program MARS10[3] which has seen extensive use in high energy deposition calculations and also has had many comparisons with other Monte Carlo programs.[4] The physics and the approach used in this program can be found in References 3 and 5.

The magnet exposures to 200 MeV protons are intended as "proof tests" of magnet coil winding methods and materials in the corrector magnet program. The described studies check parameters for run planning as well as check similar BNL calculations.[6] Only the MARS10 simulations are described here.

2.0 CALCULATIONS AND RESULTS

From detailed magnet cross section inputs MARS10 generates cross section sketches (see Figure 2a, b, and c). The numbers 1, 4, 5, and 6 indicate the following materials: Iron (Fe), coil (NbTi+Cu+Kapton), liquid helium, and insulator (G10 and/or Kapton). The magnets are all Phase I corrector magnets. The dipole and quadrupole use Texas Accelerator Center

(TAC) designed pole tips, coil shapes and apertures. The dipole is to be an ordered wind magnet, the quadrupole is a jelly roll magnet, and the sextupole is a direct wind magnet with pole tips and aperture suitable for a high energy booster (HEB). All the magnets have a beam tube diameter of 3.244 cm, typical of the Collider spool beam pipe. The coils are modelled as a continuous mixture of NbTi+Cu+Kapton (NbTi:Cu = 2.2:1) having a total density of 7.7 g/cm^3 and disregarding coil packing fractions (spaces between the wires). Therefore, one must multiply the calculated energy depositon values by the corresponding packing fraction number. In each calculation, the number of events (proton-interaction with the beam pipe) is taken as 10^5 to minimize statistical fluctuations. Therefore, the values calculated have a negligible statistical error.

Figure 3 shows the total energy deposited in the coil as a function of the square root of the beam size. A square beam was used. The abscissa, $\sqrt{A}$, is the transverse size for a beam of area A. The ordinate is the total energy deposited in the coil. The beam incident angle of interaction in this figure is $\theta = 10°$ from the magnet axis. The beam hits at the magnet midplane on one side (coil). The maximum energy concentration occurs for a point-like beam profile. Therefore, a point-like beam shape is used for energy deposition calculations (actual beams at BNL will be round beams of about 1 cm diameter).

Figure 4 shows the total energy deposited in liquid helium for the dipole and sextupole as a function of the proton-incident angle.

Figure 5a, b, and c shows the total energy deposited in the coil and the outer iron yoke lamination as a function of the proton-incident angle. More energy is deposited in the quadrupole (Q) coil and the sextupole (S) coil than in the dipole (D) coil because the thickness of Q or S coil is greater than that of the D coil. Energy deposited in the outer iron yoke lamination of D drops for $\theta > 15°$. This energy reduction is due to higher lateral and downstream energy leaks since the D outer radius is 0.895 times smaller than Q or S ($r_{\text{outer}} = 6.7$ cm) in the simulation model. Actually all coils are similar size. However, the primary effect is to the iron yoke rather than the coil. As the figures show, an angle of about 10° is a good consideration for the test experiment.

The coil is divided in 10 longitudinal sections. The model corrector lengths are taken as $L_D = 1.0$ m, $L_Q = 0.5$ m, and $L_S = 0.5$ m. Figure 6 shows their cross sectional division. The maximum energy deposited in the coil occurs in the region with the division closest to (or in) the midplane where the proton strikes. Figure 7a, b, and c shows the specific energy deposited in this region as a function of the distance along the magnet coil. The proton strikes a couple of centimeters downstream from the longitudinal start of the coil, and the specific energy reaches its maximum in about 20 cm for D, 15 cm for Q, and 13.5 cm for S, respectively. This maximum is about the same, $\epsilon_{\text{max}} \approx 5 \times 10^{-3}$ GeV/g.

Finally, Figure 8a, b, and c shows the maximum specific energy deposition, ϵ_{max}, in the midplane divisions as a function of the proton-incident angle. The saturation effect seen in ϵ_{max} for the Q and S is due to their greater thickness.

3.0 CONCLUSION

The study of the hadronic energy deposition in the superconducting corrector magnets was made for 200 MeV protons with the Monte Carlo program MARS10. The energy deposited in the coil was calculated as a function of the proton-incident angle and the beam cross section size. Hadronic shower development and energy deposition depend upon coil geometry.

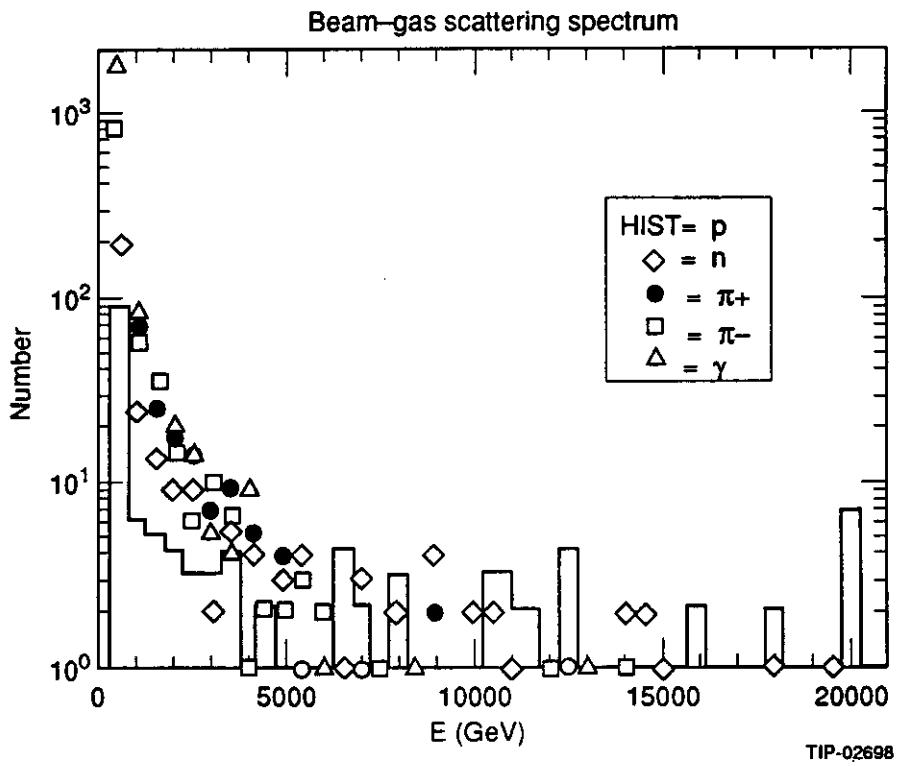

Figure 1. ISAJET 2×10^3 MB pp-events Spectrum ($\sqrt{s} = 193.7$ GeV).

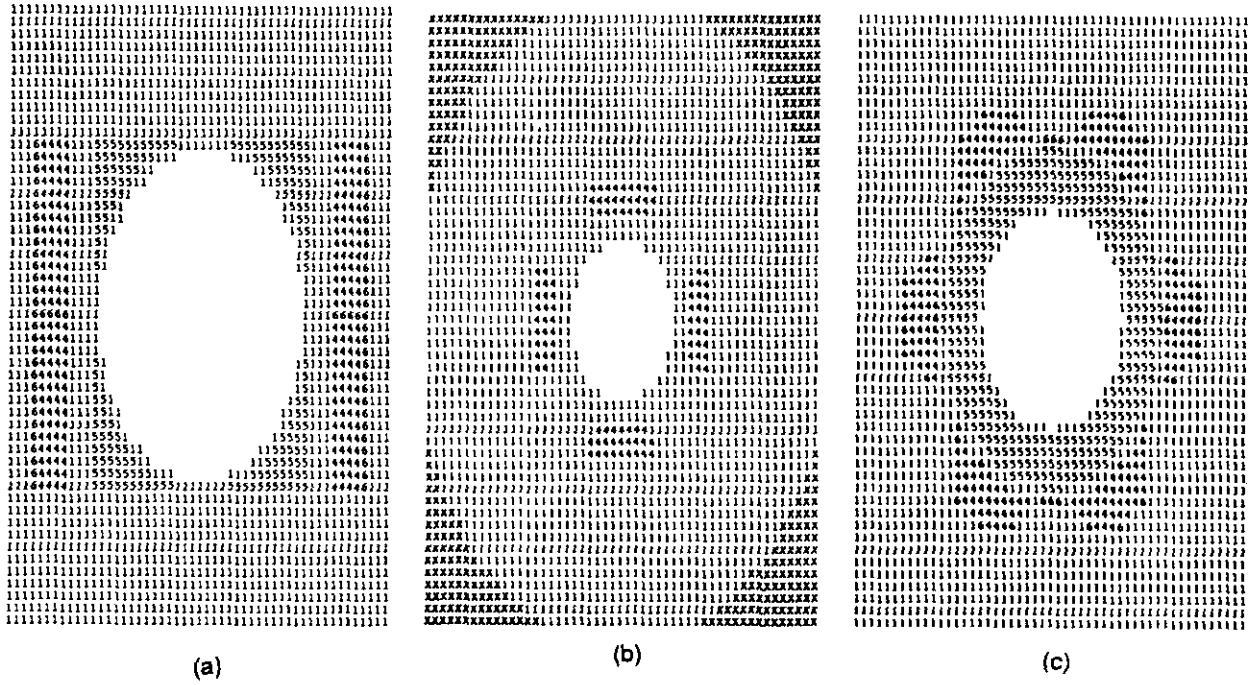

Figure 2. Cross Section of (a) Dipole Corrector Magnet, (b) Quadrupole Corrector Magnet, and (c) Sextupole Corrector Magnet.

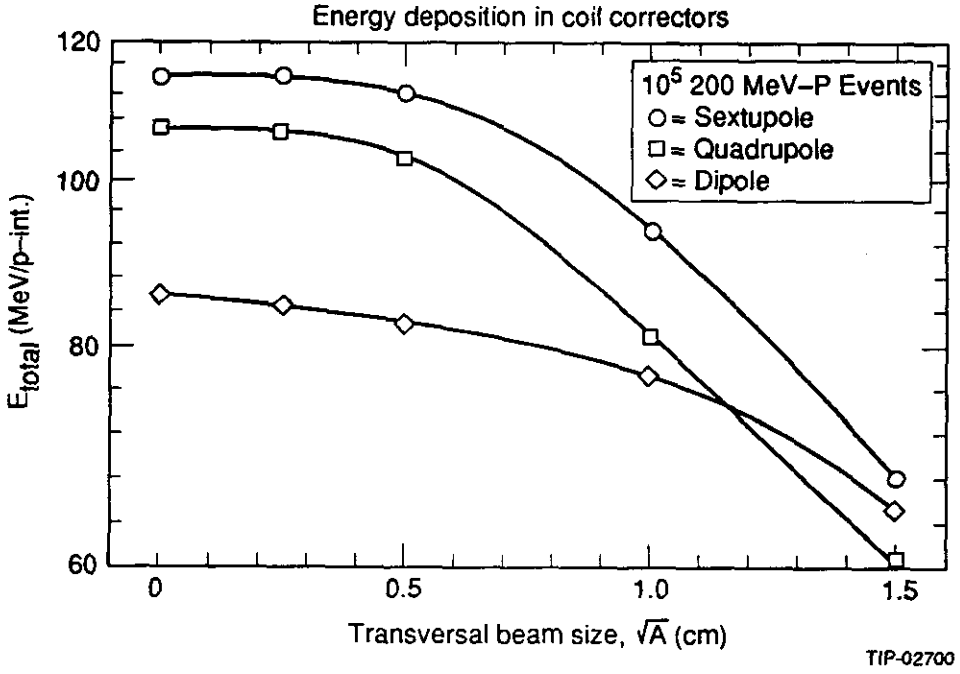

Figure 3. Total Energy Deposited in Coil vs Beam Size (Square Profile). Incident proton angle is $\theta = 10°$.

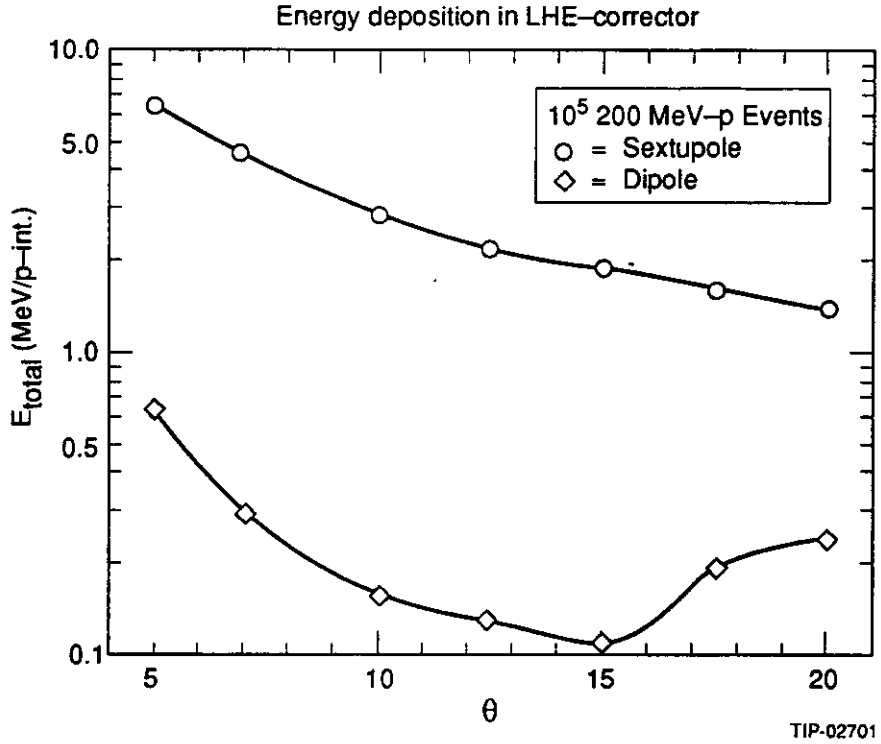

Figure 4. Energy Deposited in Liquid He vs Proton Incident Angle.

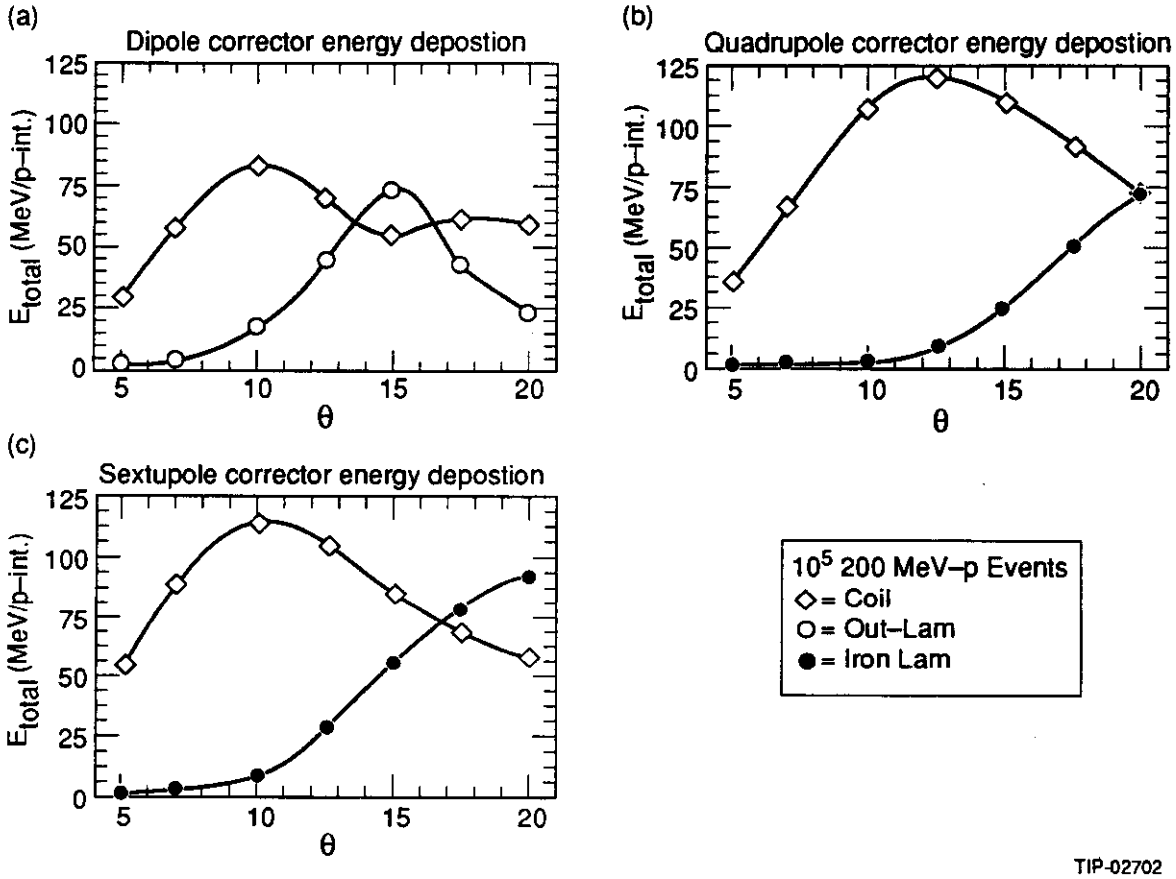

Figure 5. Total Energy Deposited in (a) the Dipole Coil and Iron Yoke, (b) the Quadrupole Coil and Iron Yoke, and (c) the Sextupole Corrector Magnet.

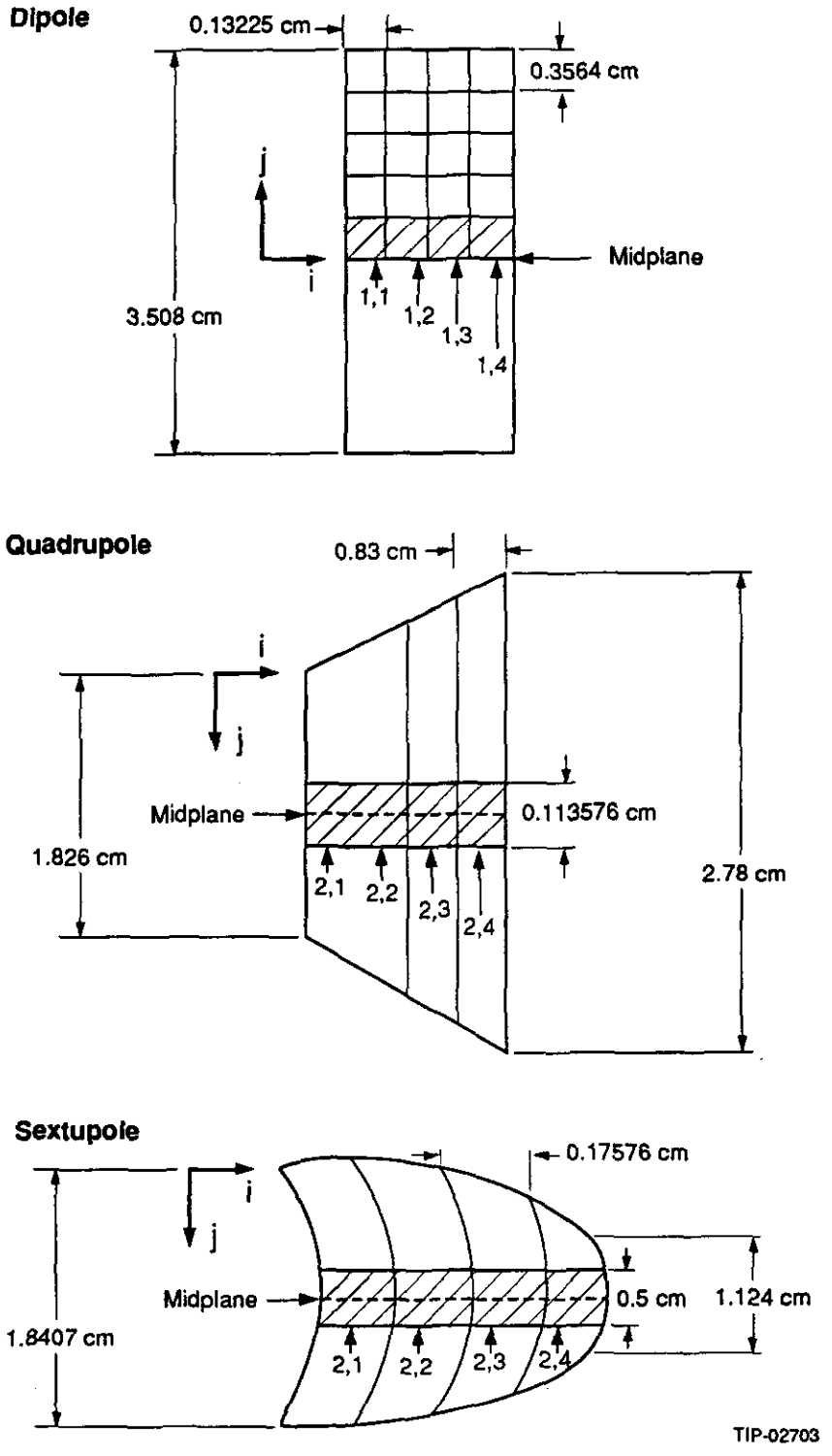

Figure 6. Cross Section Division of the Coil.

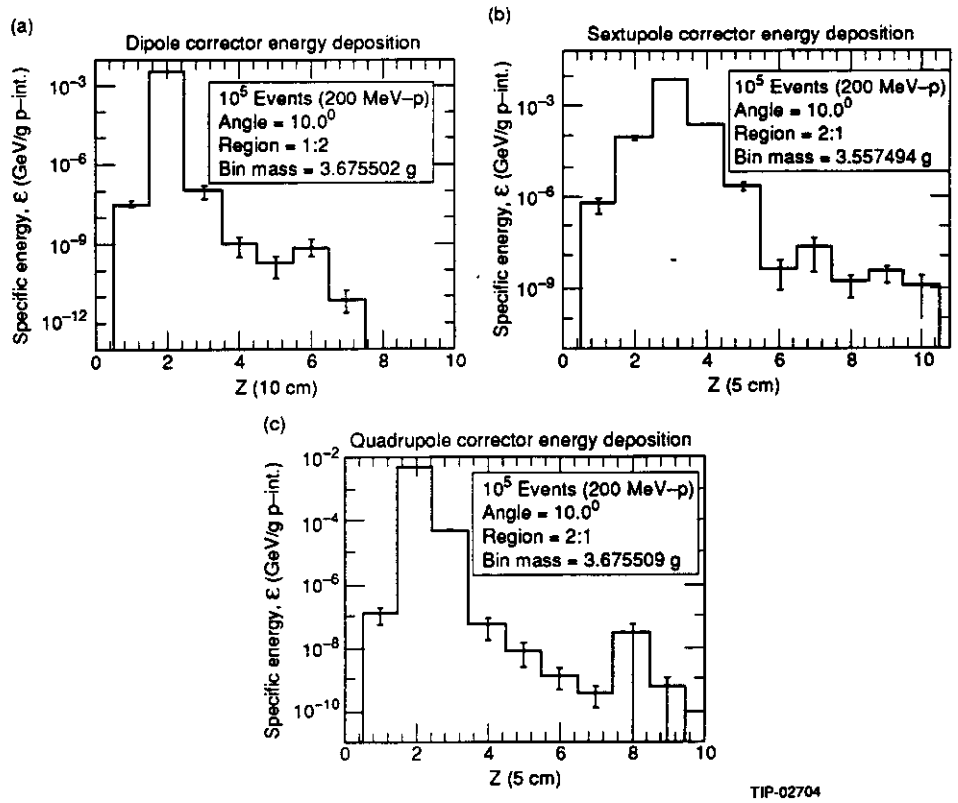

Figure 7. Specific Energy Deposited in (a) Dipole Division vs Distance (See Figure 6 for region), (b) Quadrupole Division vs Distance, and (c) Sextupole Division vs Distance.

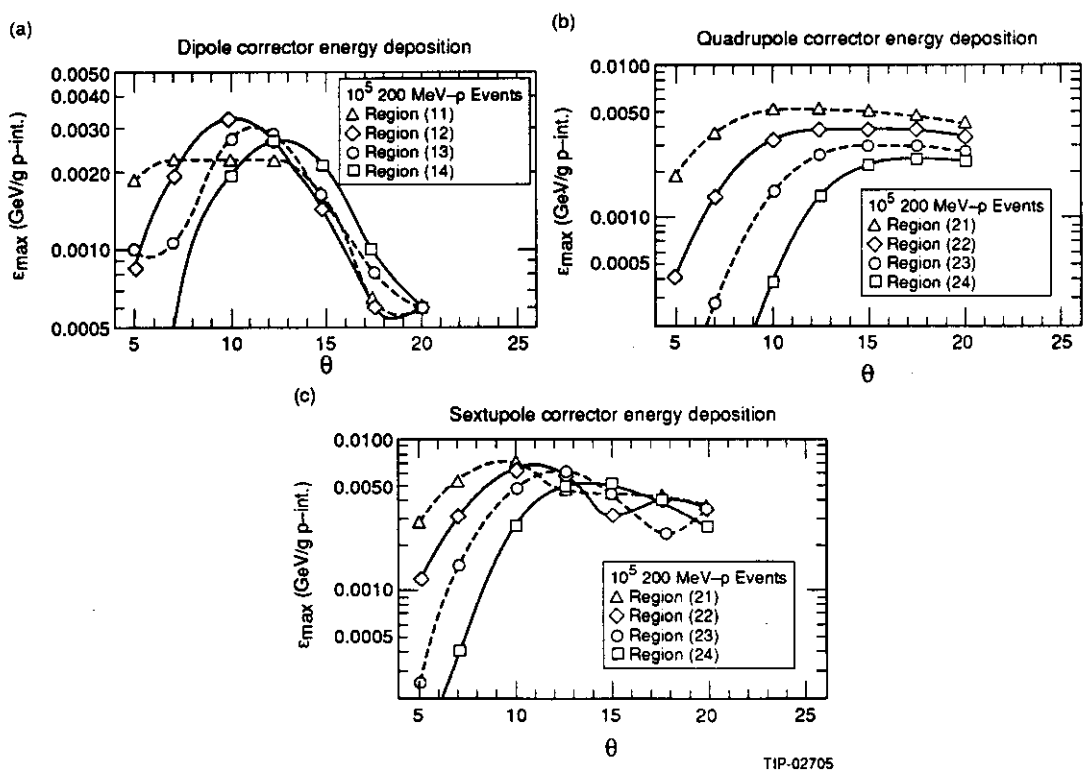

Figure 8. Maximum SED in (a) the Dipole Midplane (See Figure 6 for region), (b) the Quadrupole Midplane, and (c) the Sextupole Division vs Distance.

ACKNOWLEDGEMENTS

I wish to thank Dr. S. Stampke for his comments and suggestions, Dr. R. Schwitters, Dr. Don Edwards and D. R. Meinke for their support at the SSC Laboratory.

REFERENCES

1. N. V. Mokhov *et al.,* SSCL-306, 5 (1990).
2. N. V. Mokhov, internal communication, March 1992.
3. N. V. Mokhov, FN-509 (1989), and N. V. Mokhov. *Sov. J. Part. Nucl.* **18, 5**, 408 (1987).
4. N. V. Mokhov and J. D. Cossairt, *Nucl. Inst. Meth. in Physics Research* **A244**, 349 (1986).
5. R. P. Feynman, *Phys. Rev. Letter*, Vol. **23, 24**, 1415 (1969), and A. N. Kalinovskii, N. V. Mokhov and Yu. P. Nikitin, "Passage of High Energy Particles through Matter." American Institute of Physics AIP, N. Y. (1989).
6. M. Divadeenam uses the program LAHET at BNL.